# Chapter 6
# Spatiotemporal Variation of Snow Cover from Space in Northern Xinjiang

**Xianwei Wang, Hongjie Xie and Tiangang Liang**

**Abstract** Snow is an appreciable fraction of soil water recharge in the middle and high latitude areas, and snow cover and snow depth estimation is extremely important for regional climate change studies, agriculture and water source management. Traditional in situ measurments provide critical snow depth observations in limited areas and for ground control validation of remotely sensed estimations. Satellite-based snow measurements have revolutionized the monitoring of spatiotemporal variation of snow cover and snow depth in complex natural conditions at regional and global scales. This chaper introduces the algorithm of optical satellite snow cover detection and MODIS standard snow cover products, sumarizes recent studies on mitigating the cloud-blockage issues in MODIS snow cover products and their applications, and finally illustrates the spatiotemporal variatons of snow cover in the Northern Xinjiang, China by using the cloud-removed MODIS snow cover product. Together, snow cover days (SCD), snow cover index (SCI), snow cover onset date (SCOD) and snow cover end date (SCED) provide important information on the snow cover conditions and can be applied in any region of interests. These information would be critical for local government, such as land use planning, agriculture, live stock, and water resource management, for example, to mitigate snow-caused disasters and to plan for agriculture and industry water use. Long term availability of MODIS type of snow cover data for producing such datasets is key to study the connection between snow cover variation and climate change.

X. Wang (✉)
Center of Integrated Geographic Information Analysis,
School of Geography and Planning, and Guangdong Key Laboratory
for Urbanization and Geo-simulation, Sun Yat-sen University,
No. 135 West Xingang Road, 510275 Guangzhou, China
e-mail: xianweiw@vip.qq.com

H. Xie
Laboratory for Remote Sensing and Geoinformatics,
Department of Geological Science, University of Texas at San Antonio,
San Antonio, TX 78249, USA
e-mail: Hongjie.Xie@utsa.edu

T. Liang
College of Pastoral Agriculture Science and Technology, Lanzhou University,
No. 222 South Tianshui Road, 730020 Lanzhou, China
e-mail: tgliang@lzu.edu.cn

Y. Chen (ed.), *Water Resources Research in Northwest China,*
DOI 10.1007/978-94-017-8017-9_6, 

**Keywords** MODIS · Snow cover · Cloud removal · Northern Xinjiang

## 6.1 Introduction

Traditional in situ measurments at different climatic stations provide good snow depth observations in limited areas and are critical ground control for validating remotely sensed estimations of snow cover and snow depth. Satellite-based remote sensing snow measurements have revolutionized the monitoring of spatial and temporal distribution and variability of snow cover extent and snow depth in complex natural conditions at regional and global scales, such as those derived from the Interactive Multisensor Snow and Ice Mapping System (IMS), Scanning Multichannel Microwave Radiometer (SMMR), Special Sensor Microwave/Imager (SSM/I), Advanced Microwave Scanning Radiometer—EOS (AMSR-E), Geostationary Observational Environmental Satellite (GOES), Advanced Very High Resolution Radiometer (AVHRR), Moderate Resolution Imaging Spectraradiometer (MODIS), and Landsat (Hall et al. 2000).

Historical records of remotely sensed hemispherical snow cover maps date back to 1966, as being generated by the US National Ocean and Atmospheric Administration (NOAA) (Klein and Barnett 2003). Microwave remote sensing products, like SMMR, SSM/I, and AMSR-E, are used for global scale studies because of their high temporal resolution (daily) and with limited influence of cloud cover despite of low spatial resolution (25 km or coarser). Products derived from optical instruments using reflected solar radiation, such as AVHRR, MODIS, and Landsat, etc., have higher spatial resolution and are better for regional studies, but heavily depend on suitable weather conditions, especially clear sky (no clouds). The low temporal resolution (16 days) of Landsat data is an obstacle to its wide application in monitoring snow, even though it has much higher spatial resolution (30 m) than MODIS and AVHRR.

The Northern Xinjiang Uygur Autonomous Region is one of the three major snow distribution regions in China (Che and Li 2005; Huang and Cui 2006). Snow-related disasters frequently occur on a large scale in winter and spring, resulting in a large number of animal deaths and significant economic loss (Liu et al. 2003); meanwhile, snow is important water resources in this arid and semi-arid region. The limited ground observations revealed some temporal and minor spatial variations related to snowfall in this region over the last 50 years. However, all of the climatic stations are present in readily accessible and low elevation areas and may cause locational bias. The spatial variation of snow in mountainous and remote areas of this region may not be accurately represented in the current in situ data sets. Therefore, this chaper sumarizes the recent studies on the spatiotemporal variations of snow cover detected by the up-dated statellite technology and improved data processing methods.

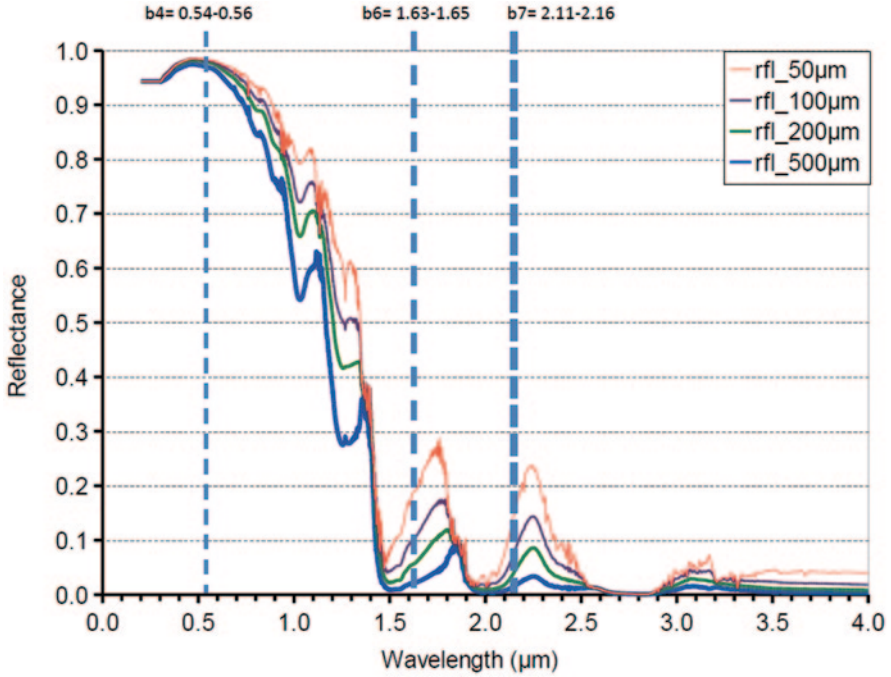


**Fig. 6.1** Predicted spectral reflectance of dry snow surface under clear sky at the Summit station (72.5794 N, 38.5042 W) of Greenland. Snow density is 250.0 kg $m^{-3}$, and snow grain radiuses are 50, 100, 200 and 500 μm from top to bottom, respectively. Finer snow grain size has higher reflectance particularly in the near and mid infrared wavelength range. Detailed model and theory description are documented by Flanner and Zender (2006). The three *dashed lines* from *left* to *right* are the wavelength positions of MODIS band 4, band 6 and band 7, respectively, and the width of the line is proportional to the width of wavelength range

## 6.2 Principles of MODIS Snow Cover Products

Snow has high reflectance in the 0.3–0.7 μm (visible) wavelength range and low reflectance for wavelengths longer than 1.4 μm (near-infrared) (Fig. 6.1). Thus, snow cover is relatively straightforward to be detected using optical remote sensing. However, challenging does exist. First, reflectance in the visible wavelengths is limited by the surface illuminated from sunlight, and low illumination and darkness cause problems, resulting in a large part of high latitude areas in winter to be omitted.

Second, electromagnetic spectrum in the visible range can not pass through cloud, and thus can not reach the land surface under cloud; another problem due to cloud is that thin cloud has similar high relfectance with snow surface in the visible range, frequently causing confusion between thin cloud and patchy snow, although most cloud has higher reflectance in the near and mid-infrared wavelength range, which is used to distinguish snow from cloud (Frei et al. 2012). Third, vegetations, particularly the dense forest canopies, obstruct visible and near-infrared signal to

reach the snow surface under canopies and reduce the snow surface albedo, making it difficult to accurately detect snow depth and extent (Klein et al. 1998; Nolin 2004). Last, surface heterogeneity, such as in mountainous areas and in the polar regions with wetlands and lakes, also makes it difficult to map snow using moderate resolution (500 m like MODIS or 1 km as AVHRR) visible and near-infrared imagery without high resolution (tens m) land surface data (Frei and Lee 2010).

### 6.2.1 MOD10A1/MYD10A1 Binary

The first MODIS standard snow cover products MOD10A1 (Terra) and MYD10A1 (Aqua) are a binary classification or hard classification, which can only tell whether it is covered by snow or not, but can not tell the snow depth and snow water equavilent (SWE). The MODIS snow-cover algorithm is based on the high reflectance of snow in the visible band (band 4 = 0.545–0.565 μm) and low reflectance in the near infrared bands (band 6 = 1.628–1.652 μm for Terra MODIS and band 7 = 2.105–2.155 μm for Aqua MODIS, due to the failure of band 6 sensor in Aqua MODIS) (Fig. 6.1). These two bands in the visible and near-infrared are used to calculate the normalized difference of snow index (NDSI) in Eq. (6.1a, b) (Hall et al. 1995).

MOD10A1:

$$NDSI = \frac{Band4 - band6}{band4 + band6} \tag{6.1a}$$

MYD10A1:

$$NDSI = \frac{Band4 - band7}{band4 + band7} \tag{6.1b}$$

Four masks are used in classifying a certain NDSI value as snow or not snow, including a dense forest stands mask, a thermal mask, a cloud mask, and an ocean and inland water mask. These masks have been incorporated in the snow cover algorithm to get the best estimation of snow. A pixel in a non-densely forested region is mapped as snow if its NDSI is $\geq 0.4$ and reflectance in MODIS band 2 (0.841–0.876 μm) is $> 11\,\%$ and reflectance in MODIS band 4 is $\geq 10\,\%$. The latter prevents pixels containing very dark targets such as black spruce forests, from being flagged as snow. The detailed algorithm and processing steps have been documented in several sources (Hall et al. 2002; Riggs et al. 2006).

### 6.2.2 MOD10A1/MYD10A1 Fractional

Accompanying with the binary snow cover products, MODIS also provides a fractional snow cover layer in the standard snow cover products (MOD10A1/MYD10A1), which are derived by using the empirical relationship between fractional snow cover and the NDSI in Eq. (6.2a, b) (Salomonson and Appel 2004, 2006; Rittger et al. 2013).

MOD10A1:

$$F_{SCA} = -0.01 + 1.45NDSI \tag{6.2a}$$

MYD10A1:

$$F_{SCA} = -0.64 + 1.91NDSI \tag{6.2b}$$

The coefficients were determined by comparing MODIS NDSI with fractional snow cover in a MODIS pixel derived from Landsat ETM+ images processed with the similar algorithm used for MOD10A1/MYD10A1 binary.

### 6.2.3 MODSCAG

Besides the MODIS standard snow cover products that are most popular in the snow community, MODSCAG (MODIS Snow Covered-Area and Grain size retrieval) algorithm has been developed to retrieve fractional snow cover as well as snow grain size based on spectral mixing analysis with MODIS spectral reflectance data (Nolin et al. 1993; Dozier and Painter 2004; Sirguey et al. 2009; Painter et al. 2009). Spectral mixture analysis is based on a set of simultaneous linear equations that are solved for the components of the pixel-averaged atmospherically corrected surface reflectance in Eq. (6.3), i.e., MODIS product MOD09GA/MYD09GA (Kotchenova and Vermote 2007).

$$R_{S,\lambda} = \sum_{K} F_k R_{\lambda,k} + \varepsilon_\lambda \tag{6.3}$$

Where $R_{s,\lambda}$ is the pixel-averaged MODIS surface reflectance in wavelength band λ; $F_k$ is the fraction of endmember k (snow, vegetation, or soil); $R_{\lambda,k}$ is the reflectance of endmember k in wavelength band λ; and $\varepsilon_\lambda$ is the residual error at λ for the fit of all endmembers. The least-squares fit to $F_k$ can be solved by several standard methods. Analysis of residuals reveals spectral regions of poor modeling and can be used for separating near-degenerate spectra (Rittger et al. 2013).

In contrast to the algorithm of MODIS standard snow cover products that rely on absolute reflectance like in Eq. (1), MODSCAG uses the relative shape of the snow's spectrum, which is sensitive to the spectral reflectance of the snow fraction. Thus, MODSCAG allows the snow's spectral reflectance to vary pixel-by-pixel and can address the spatial heterogeneity that characterizes snow and its albedo in mountainous and patchy regions. Validation and comparison study shows that it is more accurate to characterize fractional snow cover than the MODIS standard fractional snow cover algorithm based on NDSI (Rittger et al. 2013).

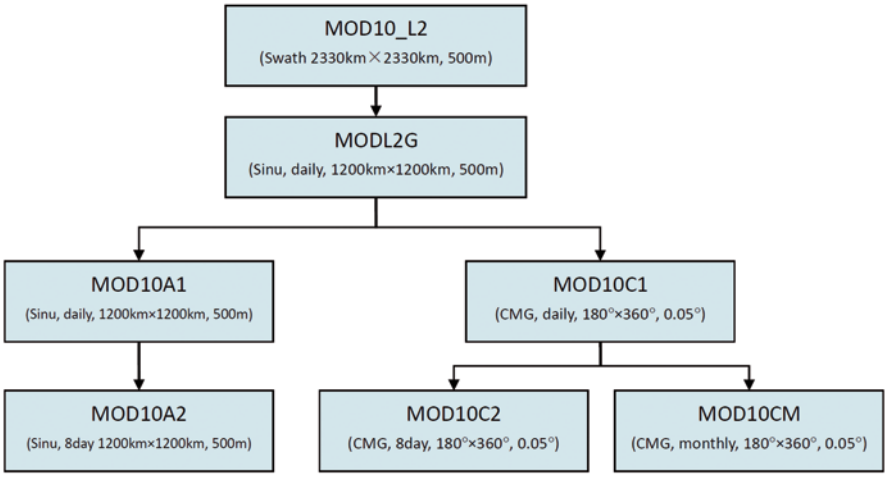


**Fig. 6.2.** Terra/Aqua MODIS standard snow cover products. Aqua MODIS snow cover product's names begin with MYD

## 6.3 MODIS Standard Snow Cover Products

Being launched on December 18, 1999, the NASA Earth Observing System (EOS) Terra satellite began collecting data on February 24, 2000 and passes the equator at about 10:30 a.m. The Aqua satellite, a counterpart of the Terra, was launched on May 4, 2002 and began collecting data on June 22, 2002. It passes the equator at about 1:30 p.m. Carried aboard the Terra and Aqua spacecrafts, MODIS standard snow cover products are produced as a series (Fig. 6.2), beginning with a swath (scene) product at a nominal pixel spatial resolution of 500 m with nominal swath coverage of 2,330 km by 2,030 km. The multiple swath observations at 500 m resolution of snow cover (MOD10_L2) are then projected onto a sinusoidal gridded tile (1,200 × 1,200 km) of MOD10L2G, which is further processed as a sinusoidal 500 m grid of daily (MOD10A1) and 8-day (MOD10A2) composite tile (1,200 × 1,200 km) products, a 0.05° global Climate Modeling Grid (CMG) daily product (MOD10C1), an 8-day product (MOD10C2), and a monthly product (MOD10CM) (Hall et al. 2002; Riggs et al. 2006; Wang et al. 2008).

Using a similar algorithm to Terra MODIS snow cover products, the Aqua MODIS also produces a parallel series of snow cover products that have a name beginning with MYD. In spite of the replacement of band 6 with band 7 in Aqua MODIS due to the failure of band 6 sensor in Aqua MODIS, both snow cover products (MOD10A1 and MYD10A1) have high agreement for cloud free snow cover classification (Wang et al. 2009).

MODIS standard snow cover products have high accuracy for clear-sky boservations and are widely applied in all kinds of studies around the world. In a validation of the MODIS swath snow product (MOD10_L2) and cloud mask in the Lower Great Lakes Regions, Ault et al. (2006) found that MOD10_L2 has very high ac-

curacy under clear sky; highest errors occur for trace snow (as snow depth < 1 cm); and the accuracy increases as snow depth increases. In a study in the eastern part of Turkey, Tekeli et al. (2005) found that the worst match between ground observations and MODIS snow cover maps was only 21 % when the sky was cloud-covered on March 24, 2004. The high frequency of cloud cover seriously impairs the accuracy of MOD10A1. In a study at the Upper Rio Grande River Basin during the 2000–2001 snow year, Klein and Barnett (2003) identified that MOD10A1 has very high overall agreement (94 %) with in situ Snowpack Telemery (SNOTEL) observations under clear skies. Most of the disagreement between MOD10A1 and SNOTEL observations occurred at the beginning and end of the snow season when thin snowpack conditions were prevalent. The high agreement between MOD10A1 and SNOTEL observation was limited to clear skies. In addition, the MODIS cloud mask appears to frequently map edges of snow-covered areas as cloud, which is likely due to lower fraction of snow (patchy snow) or thin snow depth, and thus the cloud mask requires improvement in these transition zones (Klein and Barnett 2003; Tekeli et al. 2005; Riggs et al. 2006). The fractional snow cover contained in MOD10A1 and MOD10A2 (V005) is a better representation of these transition zones (Salomonson and Appel 2004). Compared with the snow product of National Weather Service National Operational Hydrologic Remote Sensing Center (NOHRSC), MODIS classified fewer pixels as cloud than NOHRSC and significantly greater amounts of snow in the presence of clouds for topographically complex, forested, and snow-dominated areas (Maurer et al. 2003; Klein and Barnett 2003). At the same basin studied by Klein and Barnett (2003), Zhou et al. (2005) also identified clouds as a major cause affecting the accuracy of MODIS snow classification.

## 6.4 Improvements on MODIS Standard Snow Cover Products

Annually near half of the MODIS daily snow cover images are blocked by cloud, which impedes wide applications of MODIS daily snow cover products. The MODIS 8-day product (MOD10A2) minimizes cloud cover and maximizes snow cover, thereby providing better input for snowmelt runoff models. It has higher classification accuracy for both snow and land than MOD10A1 through cloud suppression. In Northern Xinjiang, China, the MOD10A2 has high accuracies under clear sky condition when mapping snow (94 %) and land (99 %) at snow depth ≥ 4 cm, but a very low accuracy (< 39 %) for patchy snow or thin snow depth (< 4 cm) (Wang et al. 2008).

Although the 8-day MODIS snow cover composites (MOD10A2/MYD10A2) greatly reduce the cloud blockage compared to daily MODIS snow cover products (MOD10A1/MYD10A1), there are more than 10 % of the MOD/MYD10A2 images where cloud coverage is more than 20 % in a year, e.g., in Northern Xinjiang, China and on the Colorado Plateau, USA (Xie et al. 2009). Moreover, the reduction of cloud with MOD/MYD10A2 sacrified their temporal resolution from daily ob-

servation to 8-day composite. In addition, the 8-day MODIS snow cover products using fixed starting and ending dates each year. This loses flexibility in monitoring particular snowfall events especially when snow can easily melt away in a few days or even in a few hours within a day, making them difficult to timely monitor the snowfall and snowmelting, particularly in the snow accumulation and snowmelting periods. Thus, the cloud issues with MODIS snow cover products severely impede wide and proper applications of MODIS standard snow cover products.

Therefore, all kinds of approaches have been developed recently to mitigate negative impacts of cloud blockage with MODIS standard snow cover products. One solution is to separate the cloud-masked pixels into "snow" or "non-snow" using a ground truth-derived ratio approach proposed by Wang et al. (2008). But this algorithm can only correct the total snow cover area and does not allow the identification of individual cloud-masked pixels as either snow or non-snow. An alternative solution is to composite multiple daily snow cover images to produce a maximum snow cover image and thereby minimize short-term environmental contaminations, like cloud, aerosol, etc. (King et al. 1992; Liang et al. 2008a), with a reduced temporal resolution. For example, the MODIS 8-day composite product (MOD10A2) reduces the original temporal resolution of daily to 8 days. A third method is using a spatial filter to replace the value of a cloud-covered pixel with the majority of its neighboring pixels' value (Parajka and Blöschl 2008). In mountainous areas, a local time-related snowline is a practical approach for estimating the cloud-covered pixels as snow or snow free (Parajka et al. 2010). Comibing the MOD/MYD10A1 with microwave estimation like AMSR-E SWE is another suitable method to fill the cloud-covered pixels, although passive microwave observations have much coarser spatial resolution and are challenging to be applied in mountainous areas (Liang et al. 2008b; Gao et al. 2010b).

The two Terra and Aqua MODIS standard snow cover products are parallel using the almost identical instrument observations and algorihtms except Aqua MODIS uses the band 7 to replace the band 6 (see Eq. 1). Since clouds are always changing in both position and extent over a three-hour period (Hall and Riggs 2007), one place (or a group of pixels) which is covered by cloud in the morning (10:30 a.m., Terra) is likely to be clear in the afternoon (1:30 p.m., Aqua), and vice versa. So, the combination of Terra and Aqua MODIS snow cover products could, in most meteorological conditions, results in cloud-less daily snow cover images and more cloud-free multi-day snow cover composite images than any single type (Terra or Aqua) of multi-day image composites. Thus, it is desirable to generate a multi-day composite image based on both Terra and Aqua MODIS daily images with flexible starting and ending dates as long as cloud cover satisfying a user-defined criterion (Wang et al. 2009; Wang and Xie 2009; Xie et al. 2009).

Taking the northern Xinjiang, China and the Colorado Plateau, USA in the 2003–2004 hydrologic year as examples, Xie et al. (2009) developed an algorithm and automated scripts to produce multi-day Terra or Aqua, and Terra-Aqua (Terra-Aqua) snow cover image composites, with flexible starting and ending dates and a user-defined cloud cover threshold. The daily composite of Terra-Aqua MODIS snow cover products has mean cloud cover ~10–15 % less than and mean snow cover

~1–4% larger than those of the daily Terra or Aqua product for the year examined. Using a cloud cover of 10% as a user-defined threshold for stopping the multiday combinations, the algorithm produced 152 and 162 multi-day Terra-Aqua composite images in the Northern Xingjiang and at the Colorado Plateau, an average of 2.4 and 2.2 days (composite period) per image, respectively. The multi-day Terra, Aqua, and Terra-Aqua composite products result in similar annual mean snow covers (~15% for the Colorado Plateau and ~30% for the northern Xinjiang) as those of the corresponding 8-day standard products, while they are ~3 times as those of the daily standard products. The multi-day Terra-Aqua composite product (average of 2–3 days composite) has much higher agreement with ground measurements than that of the standard daily products and has similar agreement as that of the standard 8-day products, but having many more images available as compared with the 46 images per year from the standard 8-day products. The new multi-day MODIS snow cover composite products (MODMYD10_MC) is a better representation of the snow cover than the standard 8-day MODIS Terra or Aqua composite alone (Wang et al. 2009). Therefore, MODMYD10_MC projects a significant contribution to the current MODIS snow cover product series and is further used to examine the spatiotemporal variation of snow cover in Northern Xinjiang, China.

Based on the daily combination of Terra and Aqua MODIS snow cover products, Hall et al. (2010) further generated a cloud-gap filled snow cover products that use previous or succeeding days' daily combination to replace the cloud-covered pixels on the current day combination to generate a near cloud-free daily snow cover image. Gao et al. (2010b) produced cloud free snow cover image and enchanced SWE product by using the daily combination of MOD/MYD10A1 and AMSR-E SWE products. We are improving our algorithm (Xie et al. 2009) to generate a daily cloud-free snow cover product, which first combines the MODIS daily Terra and Aqua snow cover products (MOD10A1 and MYD10A1) to form a daily cloudless snow cover product (MODMYD_DC), then replaces the cloud-covered pixels on the current-day MODMYD_DC with the previous-day MODMYD_DC till all cloud-covered pixels are cleared up, and finally generates a new daily cloud-free snow cover product (MODMYD_MC). The case study in Northeast China indicates that MODMYD_MC can be used to efficiently monitor the spatiotemporal variations of snow cover world around.

## 6.5 Spatiotemporal Variation of Snow Cover

Tianshan Mountains are the water tower and solid reservoir for the arid and semi-arid region in Mid Asia. The amount of rainfall and snowfall in the mountainous areas is several times higher than that in the surrounding plain, oasis and deserts. The rainfall and snow/glacier-melting runoff from the high mountains are critical recharge for the surrounding streams, lakes and groundwater. Thus, the spatiotemporal variations of snow cover are critical information for local water resource and agriculture management.

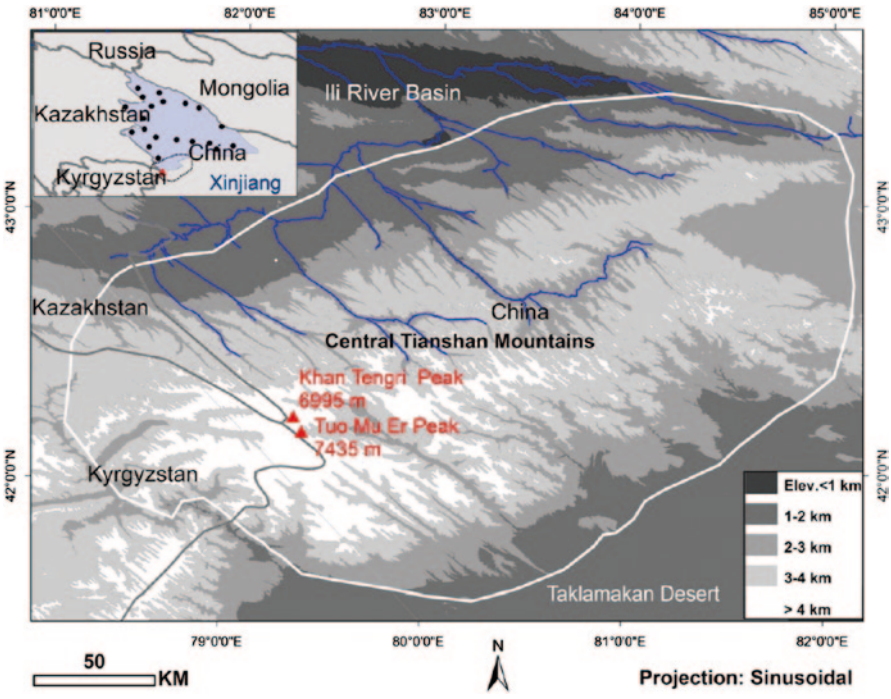


**Fig. 6.3** Test areas showing elevation distribution on central Tianshan Mountains, indicating by the *white* polygon. The shaded area on the inset map is the northern Xinjiang, China, with *black* dots for climate stations of snow depth measurements. The Ili River basin is at the north foot of Central Tianshan Mountains. The Taklamakan Desert is in the south (Source: Wang and Xie 2009)

Using the multi-day MODIS snow cover composite product MODMYD10_MC developed in Xie et al. (2009), the purpose of this session is to examine the spatiotemporal variation of snow cover and its interaction with climage change in Northern Xinjiang, China and the adjacent countries under the umbralla of two MODIS tiles of h23v04 and h24v04 (Fig. 6.3). All new maps (SCD, SCOD and SCED) are produced for the entire region of the two tiles, but the Central Tianshan Mountains is illustrated for detailed analysis as an example. Background of the figure is the elevation map from NASA's SRTM (Shuttle Radar Topography Mission) with 90 m spatial resolution. The white polygon is used to constrain the geographic region in examining the overall spatiotemporal variations of snow cover conditions by the snow cover index (SCI). The majority of the materials are edited from Wang and Xie (2009).

### 6.5.1 Definition of SCD and SCI

Snow-covered days (SCD) are calculated as the total days with snow cover at a pixel within a hydrologic year starting from Spetember 1 through next August 31 using the multi-day MODIS snow cover composite product MODMYD_MC by Eq. (6.4).

$$SCD = \sum_{i=0}^{N} (D_{i2} - D_{i1}) \tag{6.4}$$

where N is the total number of available composite images within a hydrologic year; $D_{i1}$ and $D_{i2}$ are the beginning and ending dates of each image composite, respectively. For instance, the first image composite for the hydrological year of 2003–3004 is mod03244myd03245, which is a two-day composite from MODIS Terra and Aqua, $D_{i1}=244$, $D_{i2}=245$. If a pixel value on the image is equal to 200 (e.g. with snow), the SCD value at this pixel for this image is 2. Otherwise, if the pixel value on the image is not equal to 200, the SCD value at this pixel for this image is 0. Using all composite snow cover images within a hydrologic year, we can generate a SCD map for each year, a mean SCD map for all years from 2000 to 2006 and a SCD anomaly map for each year. Using a similar algorithm, a snow cover onset date (SCOD) in fall and a snow cover end date (SCED) map in spring in each year can be generated using the cloud-low MODMYD10_MC snow cover images (Wang and Xie 2009).

Using the SCD value derived in Eq. (6.4), a snow cover index (SCI, unit: $km^2$ day) in a hydrologic year is developed to represent the overall spatial and temporal signals of snow cover conditions in a certain region and defined as Eq. (6.5).

$$SCI = \sum_{i=0}^{N} A \times SCD_i \tag{6.5}$$

where A is the area of a pixel (in $km^2$; for MODIS, the actual spatial resolution is 463 m, so $A=0.214\ km^2$); SCD(i) is the value (days) of SCD at pixel i within a hydrologic year; N is the total pixel number on an image.

### 6.5.2 Variations of Snow Cover

Compared to the SCD derived from in situ measurements at 20 climate stations in Northern Xinjiang (Figs. 6.3 and 6.4), MODIS-derived SCDs agree well (90%) with in situ SCD and are relatively higher than in situ SCDs, except for the slightly lower values at three stations (ID 979, 971, and 965). The average MODIS SCD at the 20 stations is 9 days higher than the average in situ SCD, with exceptionally much higher values at the four stations (989, 984, 988 and 973) where the MODIS SCD is about 20 days more than in situ SCD. The overall higher MODIS SCD value

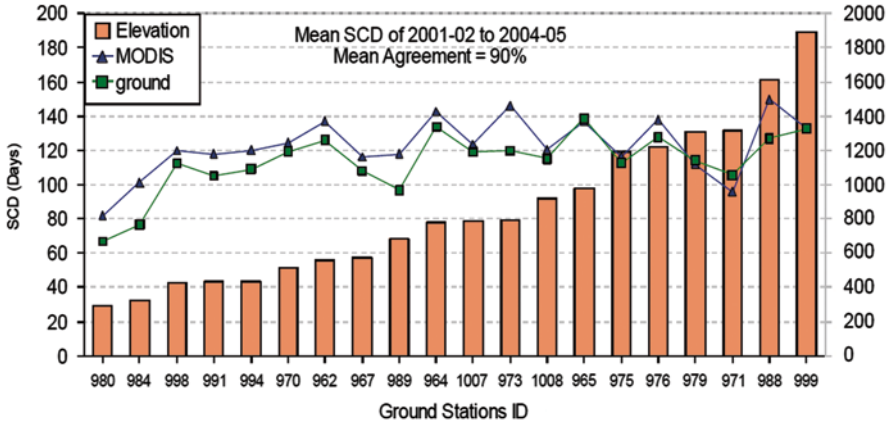


**Fig. 6.4** Comparison of MODIS mean snow covered duration/days (SCD) and in situ observations of mean SCD at 20 climate stations with ascending order of elevation (*right* scale, m) in Northern Xinjiang, China, from 2001 to 2005. The mean agreement is the average Agreements defined in Eq. (6.3) for all 20 stations in the four hydrologic year from 2001–2002 to 2004–2005. (Source: Wang and Xie 2009)

is partly due to the multi-day composite algorithm that generates maximum days of snow cover during a composite period, resulting in more snow-covered days than the daily ground measurements within a year. Another contribution to this disagreement is the comparison between point ground measurements and areal observation (500 m × 500 m) of MODIS images. The third factor is the uncertainties caused by the cloud-blocked pixels, which are about 5 % of a multi-day composite image and are ignored in calculating the SCD. In addition, other factors related to the MODIS standard daily snow cover classification, such as patchy snow, haze, dry bright sand, transition zones between snow and land, and between cloud-covered and cloud-free area, trees and forest, shaded areas by cloud, mountains, trees and buildings, and so on, also contribute to the SCD overestimation. It is also found that the agreement does not have obvious association with elevation although the relative agreements at the two lowest elevation locations (ID: 980 and 984) are larger than other locations at the higher elevations.

Figure 6.5 demonstrates the mean SCD map within the six hydrologic years on the Central Tianshan Mountains. The SCD is grouped into seven classes on a 50-days interval basis (actual SCD stretches from a few days to 365 days at individual pixels). The SCD is larger than 50 days in most of the area. Only scattered pixels in the valley, forested areas and some desert areas have less than 50 days of snow cover duration. Compared to Fig. 6.3, the SCD map is closely associated with the elevation distribution. SCDs are generally less than 100 days where elevation is lower than 1 km at the bottom of Ili River Basin and in part of the desert with elevation of 1–2 km. Dominant areas, however, have SCD from 101 to 150 days, corresponding to the 1–2 km and part of 2–3 km elevation areas. Part of the 2–3 km elevation areas has SCD of 151–250 days. Where elevations are from 3 to 4 km, SCD spans

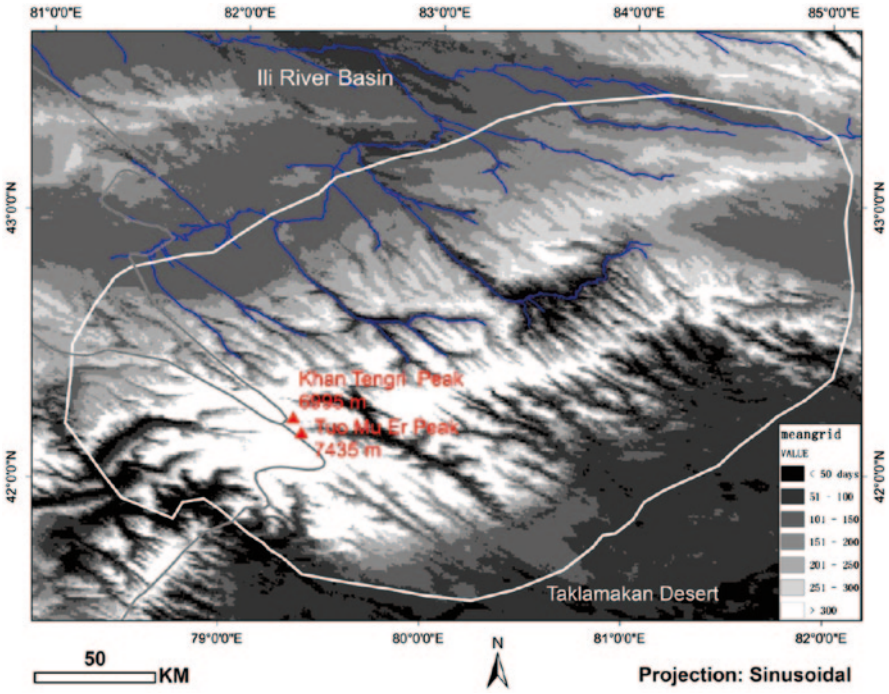


**Fig. 6.5** Spatial distribution of mean snow covered duration/days (SCD) on the Central Tianshan Mountains within the six hydrologic years from 2000 to 2006. (Source: Wang and Xie 2009)

from 200 to 300 days. At the top of the mountains where elevations are higher than 4 km, SCD is generally larger than 300 days. As the challenge in demanding snow cover maps of high temporal and spatial resolution is concerned, MODIS provides unprecedented snow cover maps and now SCD maps for various applications.

Figure 6.6 displays the spatial distribution of annual SCD difference against the mean SCD of the six hydrologic years and the minimum snow cover (or perennial snow hereafter) in August. The differences of SCD in each year have also been grouped into seven categories, i.e., $<-60$ days, $-60\sim-31$ days, $-30\sim-11$ days, $-10\sim10$ days (assumed as no change), 11–30 days, 31–60 days, and $>60$ days. One common feature of the six maps is that there is no obvious change on the top of the mountains surrounding the peak areas or the perennial snow cover. Compared to the mean SCD of the six hydrologic years, the SCD in the 2001–2002 and 2004–2005 hydrological years had overall higher values than the mean. In contrast, both 2003–2004 and 2005–2006 years had lower values than the mean in most of the areas, especially in 2005–2006 year.

Figure 6.7 shows the quantitative variation of overall snow cover conditions as indicated by SCI on the Central Tianshan Mountains. It has a similar pattern with Fig. 6.6 that 2001–2002 and 2004–2005 have higher SCD values than the mean SCD of the 6 years, resulting much higher SCI in the 2 years than other

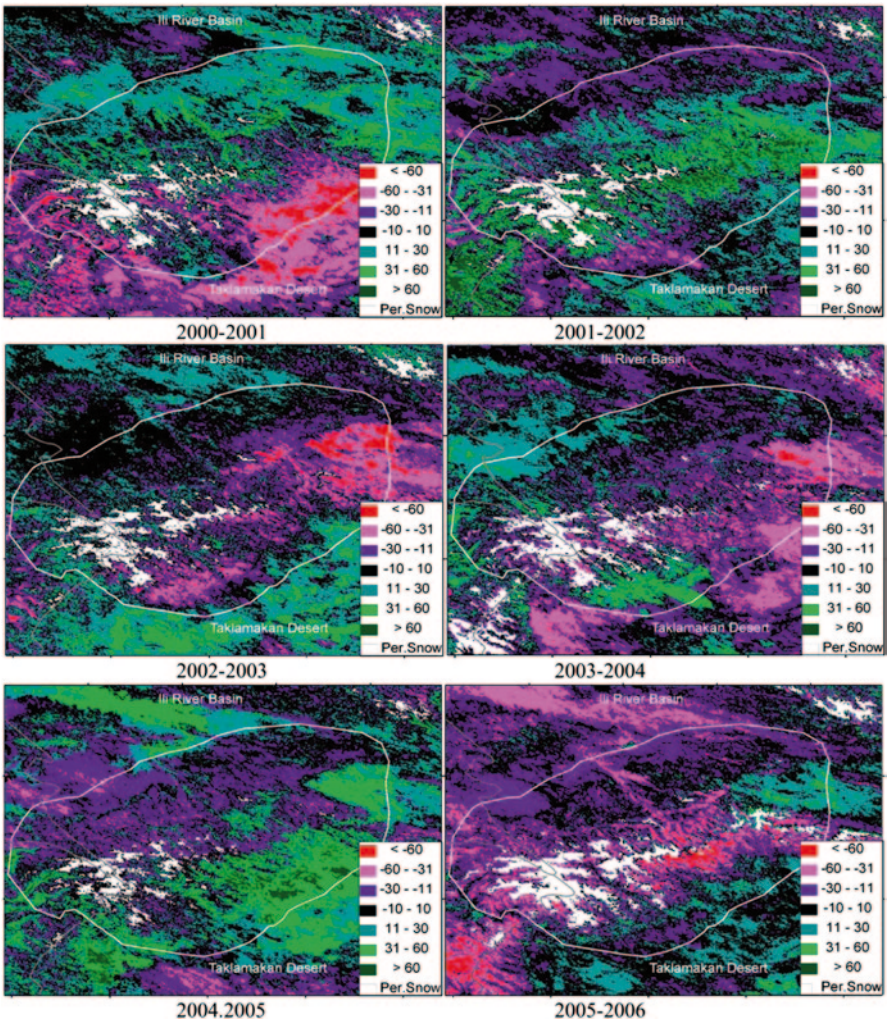


**Fig. 6.6** Spatial distribution of SCD anomaly map in each hydrological year on the Central Tianshan Mountains. The mean SCD map of the 6 years was used as a basis. The *white* area represents the minimum snow cover or perennial snow in August of each year. (Source: Wang and Xie 2009)

years. The reverse patterns in Fig. 6.6 between 2000–2001 and 2004–2005, and between 2001–2002 and 2002–2003, are also quantified at a similar reverse pattern in Fig. 6.7. The 2 years in 2003–2004 and 2005–2006 have lower SCD distributions than mean SCD in Fig. 6.6, leading to similar lower SCIs than the other years. SCI in this short period (2001–2006) does not show any obvious trend. The longer records of snow cover products using NOAA's AVHRR data may provide a better change trend of snow cover in the recent 30 years. The continuing MODIS data is

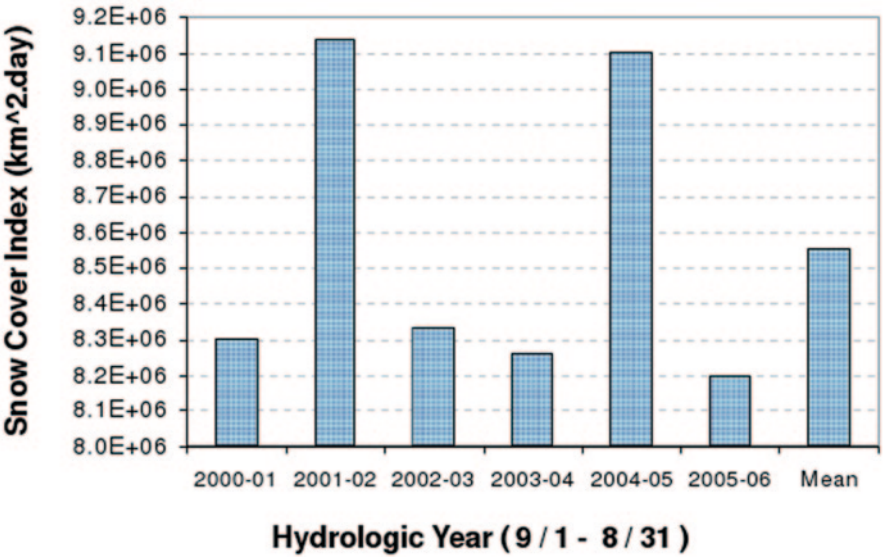


**Fig. 6.7** Variation of snow cover index (SCI) on the Central Tianshan Mountains within the six hydrologic years from 2000 to 2006. (Source: Wang and Xie 2009)

also critical to monitor the change trend of the snow cover conditions at this region and other regions of the world.

Figure 6.8 illustrates the spatial distribution of snow cover onset dates (SCOD) and end dates (SCED) maps on the Central Tianshan Mountains in the fall and spring seasons of 2004 and 2005, respectively. The SCOD values are categorized into seven classes: before (<) September 15 (or O1), September 16–30 (O2), October 1–15 (O3), October 16–31 (O4), November 1–15 (O5), November 16–30 (O6), and after (> December 1 (O7). Similar to SCOD, the SCED values are also categorized into seven classes: after (>) May 1 (or E1), April 16–30 (E2), April 1–15 (E3), March 16–31 (E4), March 1–15 (E5), February 16–28 or 29 (E6), and before (<) February 15 (E7). While Figs. 6.5, 6.6 and 6.7 respectively give the general spatial distribution of the mean SCD in the 6 hydrologic years, the SCD anomalies against the mean SCD and the overall snow cover conditions (SCI) in each year, Fig. 6.8 furthern provides the spatial distribution of the specific dates when the snow cover begins and when the snow cover melts away at the scale of one MODIS pixel (500 m), respectively. Taking the 2004–2005 and 2005–2006 two hydolgic years as examples, Fig. 6.8 explains the reasons that formed the contrast of SCD variations in 2004–2005 and in 2005–2006 in the Ili River Basin, i.e., similar SCOD in 2004 Fall and in 2005 Fall, but SCED is in April 16–30 in 2005 Spring vs SCED mostly in March 1–15 in 2006 Spring, leading to 30–60 shorter SCD in 2005–2006 than that in 2004–2005. Similar patterns exist in the Southeast of Central Tianshan Mountains in these two hydrologic years (Wang and Xie 2009).

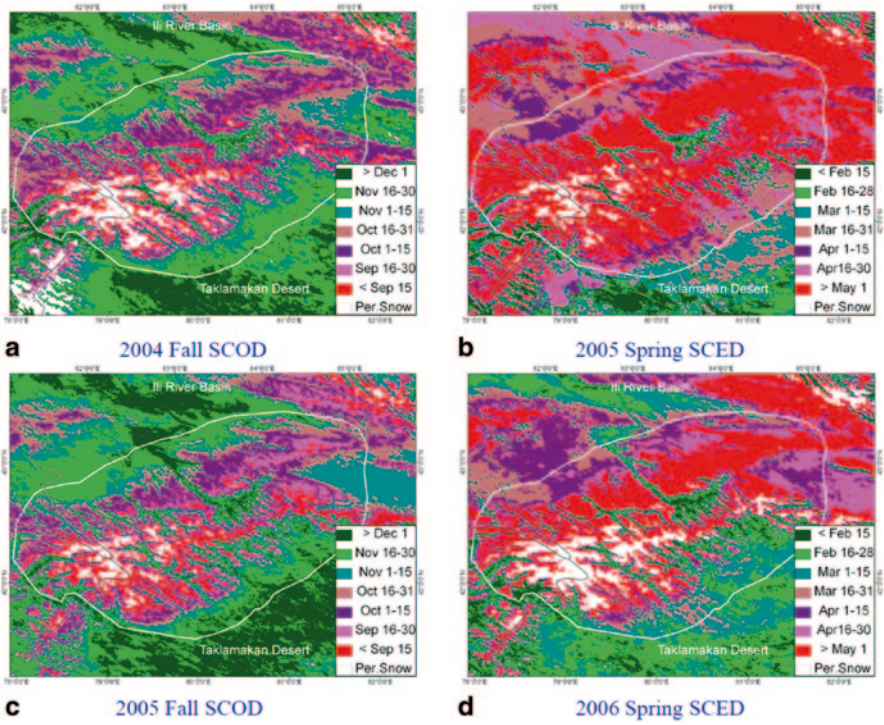


**Fig. 6.8** Spatial distribution of snow cover onset dates (SCOD) and end dates (SCED) maps on the Central Tianshan Mountains in the fall and spring seasons of 2004 and 2005, respectively. The *white* area represents the minimum snow cover or perennial snow in August of each year. (Source: Wang and Xie 2009)

### *6.5.3 Variations of Perrenial Snow and Glacier*

The spatial distribution of perennial snow is illustrated on Figs. 6.6 and 6.8. The perennial snow cover had similar spatial distribution pattern on the top of the high-elevation (>4 km) mountains in spite of yearly variation. The perennial snow cover in each year did not vary at the same trend with the overall snow cover duration. For example, on Fig. 6.6, although 2003–2004 and 2005–2006 has overall lower SCD, their perennial snow cover shown in August of 2004 and 2006 has larger areas than other years, especially in the August of 2004 when there only appeared snow cover at the southwest corner of the map in the 6 years. The 2004–2005 had overall higher SCD, but its perennial snow cover shown in the August of 2005 had the least snow cover extent in the six hydrologic years. This least snow cover extent is assumed to represent the maximum glacier distribution since it is difficult to distinguish perennial snow cover from glacier using the MODIS snow cover products. Perennial snow/glacier cover mainly distributes on the top of the mountains with elevation >4 km and has a spatial extent ~2,380 km$^2$ according to the least perennial snow

cover map in the August of 2005. More accurate map of glacier distribution at this region can be obtained using Landsat or other higher resolution images (Li et al. 2004). Further study will examine the glacier coverage and its elevation (volume) change through integrating accurate laser elevation measurements (i.e. ICESat) (Wang and Xie 2009).

**Summary and remarks** Snow cover and snow depth estimation is extremely important for regional climate change studies, agriculture and water source management. Satellite-based snow measurements have revolutionized the monitoring of spatiotemporal variation of snow cover and snow depth in complex natural conditions at regional and global scales. This chaper introduces principles of optical satellite snow cover detection and the MODIS standard snow cover products, sumarizes recent efforts on mitigating the cloud-blockage issues in the optical snow cover detections and its applications, and finally illustrates the spatiotemporal variatons of snow cover in the Central Tianshan Mountains mostly in Northern Xinjiang, China by using the cloud-removed MODIS snow cover product.

Overall, MODIS standard snow cover products have high accuracy for clear-sky observations and are widely applied in all kinds of studies around the world. In contrast, MODSCAG uses the relative shape of the snow's spectrum and is more accurate to characterize fractional snow cover than the MODIS standard snow cover products (Rittger et al. 2013). However, the impact of this improvement for fractional snow cover on the total water resource budget is limited. Meanwhile, cloud blockage severely obstacles the wide application of MODIS daily snow cover products. All kinds of efforts have been done to mitigate the negetive effects of cloud cover.

Benefiting from daily twice observations of Terra and Aqua MODIS sensors and the parallel MODIS snow cover products in the morning and afternnoon, the flexible multi-day MODIS snow cover composite products MODMYD10_MC is a better representation of the snow cover than the standard 8-day MODIS Terra or Aqua composite alone, and is further used to examine the spatiotemporal variation of snow cover on the Central Tianshan Mountains using all kinds of snow mapping methods (Wang et al. 2009; Wang and Xie 2009).

While an SCD map gives the overall spatial distribution of snow cover duration, both SCOD and SCED maps provide the spatial distribution of the specific dates when the snow cover starts and when the snow cover melts away at the pixel scale of 500 m. Together, SCD, SCI, SCOD and SCED provide important information on the snow cover conditions and can be applied in any region of interests. This information could be critical for local government, such as land use planning, agriculture, live stock, and water resource management, for example, to mitigate snow-caused disasters and to plan for agriculture and industry water use. Long term availability of MODIS type of snow cover data for producing such datasets is key to study the connection between snow cover variations and climate change. For example, possible applications for this data are to study the relation between SCI and annual (hydrologic year) mean temperature change, to study the relation between SCI and El Nino-Southern Oscillation (ENSO), and to examine the time series change of

annual mean SCD, SCOD and SCED for a region. Additional questions can also be addressed through the type of data presented. Does global warming reduce the mean snow cover days for a region? Does global warming have potential to forward shift or backward shift the mean snow cover onset date and/or mean snow cover melting date? How does the spring sand-storm or dust soil from the south desert impact the melting of snow cover?

## References

Che T, Li X (2005) Spatial distribution and temporal variation of snow water resources in China during 1993–2002. J Glaciol Geocryol 27(1):64–67. (In Chinese)

Dozier J, Painter TH (2004) Multispectral and hyperspectral remote sensing of alpine snow properties. Ann Rev Earth Planet Sci 32:465–494

Flanner MG, Zender CS (2006) Linking snowpack microphysics and albedo evolution. J Geophys Res 111:D12208. doi:10.1029/2005JD006834

Flerchinger GN, Cooley KR, Ralston DR (1992) Groundwater response to snowmelt in a mountainous watershed. J Hydrol 133(3-4):293–300

Frei A, Lee S (2010) A comparison of optical-band based snow extent products during Spring over North America. Remote Sens Environ 114:1940–1948

Frei A, Tedesco M, Lee S, Foster JL, Hall DK, Kelly RE, Robinson DA (2012) A review of global satellite-derived snow products. Adv Space Res 50:1007–1029

Gao Y, Xie H, Yao T et al (2010a) Integrated assessment on multi-temporal and multi-sensor combinations for reducing cloud obscuration of MODIS snow cover products of the Pacific Northwest USA. Remote Sens Environ 114:1662–1675

Gao Y, Xie H, Lu N, Yao T, Liang T (2010b) Toward advanced daily cloud-free snow cover and snow water equivalent products from Terra-Aqua MODIS and Aqua AMSR-E measurements. J Hydrol 385:23–35

Hall DK, Riggs GA (2007) Accuracy assessment of the MODIS snow-cover products. Hydrol Process 21:1534–1547

Hall DK, Riggs GA, Salomonson VV (1995) Development of methods for mapping global snow cover using moderate resolution imaging spectroradiometer data. Remote Sens Environ 54:127–140

Hall DK, Tait AB, Foster JL, Chang ATC, Allen M (2000) Inter comparison of satellite-derived snow-cover maps. Ann Glaciol 31:369−376

Hall DK, Riggs GA, Salomonson VV et al (2002) MODIS snow-cover products. Remote Sens Environ 83:181–194

Hall DK, Riggs GA, Foster JL et al (2010) Development and evaluation of a cloud-gap-filled MODIS daily snow-cover product. Remote Sens Environ 114:496–503

Huang Z, Cui C (2006) Snow monitoring using EOS/MODIS data in Xinjiang, China. J Glaciol Geocryol 28(3):343–347. (In Chinese)

Kanneganti VR, Bland WL, Undersander DJ (1998) Modeling freezing injury in Alfalfa to calculate forage yield: II. Model validation and example simulations. Agron J 90:698–704

King MD, Kaufman YJ, Menzel WP, Tanre D (1992) Remote sensing of cloud, aerosol, and water vapor properties from the Moderate Resolution Imaging Spectrometer (MODIS). IEEE Trans Geosci Remote Sens 30(1):2–27

Klein AG, Barnett AC (2003) Validation of daily MODIS snow cover maps of the Upper Rio Grande River Basin for the 2000–2001 snow year. Remote Sens Environ 86:162–176

Klein AG, Hall DK, Riggs GA (1998) Improving snow cover mapping in forests through the use of a canopy reflectance model. Hydrol Process 12:1723–1744

Kongoli CE, Bland WL (2000) Long-term snow depth simulations using a modified atmosphere-land exchange model. Agric Forest Meteorol 104:273–287
Kotchenova SY, Vermote EF (2007) Validation of a vector version of the 6S radiative transfer code for atmospheric correction of satellite data. Part II.Homogeneous Lambertian and anisotropic surfaces. Appl Opt 46:4455–4464
Liang TG, Huang XD, Wu CX, Liu XY, Li WD, Guo ZG, Ren JZ (2008a) An application of MODIS data on snow cover monitoring in pastoral area: a case study in the Northern Xinjiang, China. Remote Sens Environ 112:1514–1526
Liang TG, Zhang XT, Xie HJ, Wu CX, Feng QS, Huang XD, Chen QG (2008b) Toward improved daily snow cover mapping with advanced combination of MODIS and AMSR-E measurements. Remote Sens Environ 112:3750–3761
Liu X, Liang T, Guo Z, Li L (2003) Assessment and monitoring of snow disaster effect on grassland livestock industry in the Aletai region using remote sensing technology. Acta Pratalculturae Sinica 12(6):115–119. (In Chinese)
Maurer EP, Rhoads JD, Dubayah RO, Lettenmaier DP (2003) Evaluation of the snow covered area data product from MODIS. Hydrol Process 17:59–71
Nolin AW (2004) Towards retrieval of forest cover density over snow from the Multi-angle Imaging SpectroRadiometer (MISR). Hydrol Process 18:3623–3636
Nolin AW, Dozier J, Mertes LAK (1993) Mapping alpine snow using a spectral mixture modeling technique. Ann Glaciol 17:121–124
Painter TH, Rittger K, McKenzie C, Slaughter P, Davis RE, Dozier J (2009) Retrieval of subpixel snow covered area, grain size, and albedo from MODIS. Remote Sens Environ 113:868–879
Parajka J, Blöschl G (2008) Spatio-temporal combination of MODIS images-potential for snow cover mapping. Water Resour Res 44:W3406
Parajka J, Pepe M, Rampini A, et al (2010) A regional snow-line method for estimating snow cover from MODIS during cloud cover. J Hydrol 381:203–212
Riggs GA, Hall DK, Salomonson VV (2006) MODIS Snow Products User Guide to Collection 5, Online article. http://modis-snow-ice.gsfc.nasa.gov/userguides.html. Accessed 2 Jan 2007
Rittger K, Painter TH, Dozier J (2013) Assessment of methods for mapping snow cover from MODIS. Adv Water Resour 51:367–380
Rodell M, Houser PR (2004) Updating a Land Surface Model with MODIS-derived snow cover. J Hydrometeorol 5:1064–1075
Salomonson VV, Appel I (2004) Estimating fractional snow cover from MODIS using the normalized difference snow index. Remote Sens Environ 89:351–360
Salomonson VV, Appel I (2006) Development of the Aqua MODIS NDSI fractional snow cover algorithm and validation results. IEEE Trans Geosci Remote Sens 44:1747–1756
Sirguey P, Mathieu R, Arnaud Y (2009) Sub-pixel monitoring of the seasonal snow cover with MODIS at 250 m spatial resolution in the Southern Alps of New Zealand: methodology and accuracy assessment. Remote Sens Environ 113:160–181
Tekeli EA, Akyurek Z, Sorman AA, Sensoy A, Sorman AU (2005) Using MODIS snow cover maps in modeling snowmelt runoff process in the eastern part of Turkey. Remote Sens Environ 97:216–230
Wang X, Xie H (2009) New methods for studying the spatiotemporal variation of snow cover based on advanced combination products of MODIS Terra and Aqua. J Hydrol 371:192–200
Wang X, Xie H, Liang T (2008) Evaluation of MODIS Snow Cover and Cloud Mask and its Application in Northern Xinjiang, China. Remote Sens Environ 112:1497–1513
Wang X, Xie H, Liang T, Huang X (2009) Comparison and validation of MODIS standard and new combination of Terra and Aqua snow cover products in Northern Xinjiang, China. Hydrol Process 23:419–429. doi:10.1002/hyp.7151
Xie H, Wang X, Liang T (2009) Development and assessment of combined Terra and Aqua MODIS snow cover products in Colorado Plateau, USA and northern Xinjiang, China. J Appl Remote Sens 3(033559):1–14

Zhou L, Li H, Wang Q (2000) The basic characteristics of heavy snowstorm process and snow disaster distribution in eastern pastoral areas of Qinghai-Xizang Plateau. Plateau Meterol 19(4):450–458. (In Chinese)

Zhou L, Wang Q, Li H, Zhang H, Li J (2001) Study on real-time predictive assessment of snow-storm disaster in eastern pastoral area of Qinghai-Tibet Plateau. J Nat Disasters 10(2):58–65. (In Chinese)

Zhou X, Xie H, Hendrickxa MHJ (2005) Statistical evaluation of remotely sensed snow-cover products with constraints from streamflow and SNOTEL measurements. Remote Sens Environ 94:214–231